

5-2015

Computational Analysis of the Maximum Optical Enhancement of Gold Nanowires and Nanowire Arrays

Cole Cameron Saylor
University of Arkansas, Fayetteville

Follow this and additional works at: <https://scholarworks.uark.edu/physuht>



Part of the [Physics Commons](#)

Citation

Saylor, C. C. (2015). Computational Analysis of the Maximum Optical Enhancement of Gold Nanowires and Nanowire Arrays. *Physics Undergraduate Honors Theses* Retrieved from <https://scholarworks.uark.edu/physuht/2>

This Thesis is brought to you for free and open access by the Physics at ScholarWorks@UARK. It has been accepted for inclusion in Physics Undergraduate Honors Theses by an authorized administrator of ScholarWorks@UARK. For more information, please contact scholar@uark.edu, uarepos@uark.edu.

Computational Analysis of the Maximum Optical Enhancement of Gold Nanowires and Nanowire Arrays

An Undergraduate Honors College Thesis

in the

Department of Mechanical Engineering
College of Engineering
University of Arkansas
Fayetteville, AR

By

Cameron Saylor

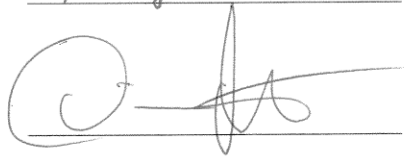
This thesis is approved.

Thesis Advisor:

 _____

Thesis Committee:

 _____

 _____

ABSTRACT

Plasmonic devices have gained popularity recently due to their unique ability to focus light to scales smaller than the diffraction limit and amplify the intensity of incident light. One such plasmonic device is the gold nanowire, a simple geometry that can be fabricated into a variety of geometric patterns. The aim of this project was to determine the effect of nanowire geometry on its maximum optical enhancement. For this purpose, the plasmonic optical enhancement properties of single gold nanowires and triple nanowire arrays were investigated using finite element method simulations. The results of the simulations indicate a significant effect on the optical enhancement of both the thickness and width of the nanowires. From the simulation data, an equation for each geometry (single and triple array) was found that relates the dimensions and incident wavelength to the optical enhancement. These equations can be used while designing nanowires to optimize the dimensions and provide the maximum possible optical enhancement.

TABLE OF CONTENTS

Figures.....	i
Acknowledgments.....	ii
Chapter 1: Introduction.....	1
1.1 Plasmons.....	1
1.2 Applications of Plasmons.....	2
1.3 Motivation.....	2
Chapter 2: Plasmonics Simulations.....	4
2.1 Experimental Methods.....	4
2.2 Interpreting Results.....	6
Chapter 3: Results.....	7
3.1 Single Nanowire Width Dependence.....	7
3.2 Triple Nanowire Array.....	9
3.3 Thickness Dependence.....	13
Chapter 4: Conclusion.....	18
Appendix A: Performing a Simulation in COMSOL.....	19
Appendix B: MATLAB Code Used to Generate Color Plots.....	24
Bibliography.....	25

FIGURES

Figure 1: Diagram of the free electron oscillation caused by interaction with an incident electromagnetic wave.

Figure 2: A screenshot displaying the mesh used to perform FEM simulations of a single 2D gold nanowire. The area surrounding the nanowire geometry is the far field domain. The darker rectangles surrounding the edges of the nanowire are included to allow the calculation of average enhancement inside, but are not used in this paper.

Figure 3: (a) Enhancement spectrum and (b) electric field distributions for single gold nanowires of varying widths.

Figure 4: (a) Wavelength of maximum enhancement and (b) FWHM of enhancement spectrum as functions of width for a single nanowire.

Figure 5: (a) Triple nanowire array geometry, (b-d) enhancement distributions of triple nanowire arrays with various geometries.

Figure 6: Maximum enhancement of triple nanowire array as a function of w_s and w_L for triple nanowire array.

Figure 7: (a) Maximum optical enhancement as a function of w_s and (b) w_L as a function of w_s for triple nanowire array.

Figure 8: Maximum optical enhancement as a function of width and thickness for a single nanowire.

Figure 9: (a) Thickness showing maximum enhancement as a function of width and (b) maximum enhancement as a function of width.

Figure 10: Electric field distributions of single nanowires of varying thickness.

ACKNOWLEDGMENTS

I would like to thank Dr. Joseph Herzog for his mentorship and support throughout the time spent on this project. I would also like to acknowledge Avery Hill for helping me learn to use COMSOL, Eric Novak for providing his models that served as a base to begin this project and Desalegn Debu for providing some of the figures in this paper.

I would like to thank Dr. Joseph Herzog, Dr. Gay Stewart, Dr. Larry Roe, Dr. Darin Nutter and Dr. T.K.S. Kumar for serving on my thesis committee, and Dr. Doug Spearot for serving as my mechanical engineering thesis adviser.

CHAPTER 1:

INTRODUCTION

1.1 Plasmons

The field of plasmonics is concerned with studying the interaction between the free electrons in a metal and electromagnetic waves. Plasmons have attracted attention due to their ability to focus light to scales smaller than the diffraction limit. Advancements in nanofabrication techniques have made it possible to manufacture structures with features on the scale of nanometers; a scale extremely useful for plasmonic nanostructures. In the subwavelength length scale, the free electrons in metallic nanostructures exhibit interesting interactions with electromagnetic waves.

When an electromagnetic wave is incident on a metal surface, it will cause an oscillation of the free electron density of the metal. The oscillation of these electrons is quantized, and this quantization of plasma oscillations is called a plasmon¹. Because plasmons are a quantization of plasma oscillations, their properties can be derived from Maxwell's equations². The oscillation of the free electrons caused by incident electromagnetic waves is depicted in Fig. 1.

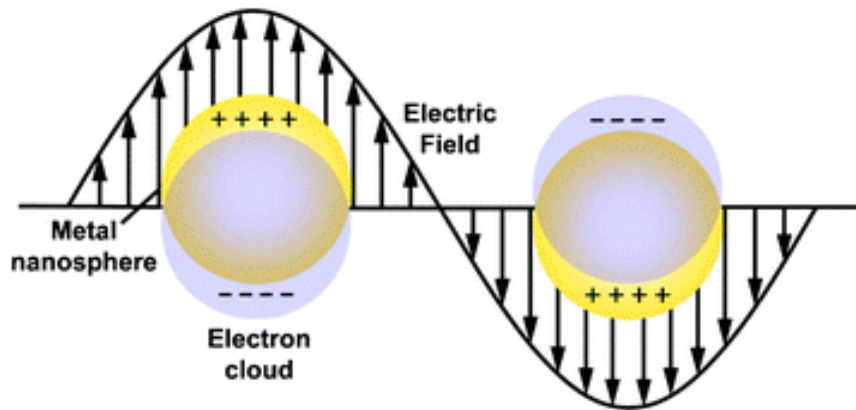


Fig. 1 Diagram of the free electron oscillation caused by interaction with an incident electromagnetic wave.³

1.2 Applications of Plasmons

The usefulness of plasmons is exhibited by their ability to localize light to scales much smaller than the diffraction limit⁴ and amplify the magnitude of the electric field in plasmonic nanostructures to many times more than the incident electric field. Plasmonic structures exhibit polarization,⁵ incident wavelength and nanostructure geometry dependence⁴, so the maximum possible electric field amplification will vary for any given plasmonic coupling conditions. The importance in proper tuning of plasmonic properties becomes apparent in the wide variety of possible applications for plasmonic devices, such as: enhanced photovoltaics,^{6,7} biosensing,⁸ surface-enhanced Raman spectroscopy,⁹ enhanced photodetectors,^{7,10-12} thermoplasmonic applications¹³⁻¹⁵ and photothermal therapy¹⁶⁻¹⁹. These applications have potentially significant impact across many societally important issues, from improved energy production to medical treatment.

1.3 Motivation

This work will investigate a variety of geometric configurations in gold nanostructures to optimize the plasmonic enhancement properties of the devices. The

purpose of the following simulations is to maximize the achievable optical enhancement due to plasmonic coupling of electromagnetic waves with gold nanowires. Maximizing the optical enhancement of gold nanowires will improve their performance in the above listed applications and perhaps even open up new applications that were not previously possible. Similar goals have been presented in previous work,^{18,20} but are more specific in scope or differ in the investigated geometry. This work attempts to find a general relationship between nanowire geometry and optical enhancement, to provide a base from which more specific investigations and applications can start. One such application that motivated the investigation of triple nanowire arrays is the use of nanogaps to improve surface-enhanced Raman spectroscopy²¹.

CHAPTER 2: PLASMONICS SIMULATIONS

2.1 Experimental Methods

Optical studies have been performed on a variety of gold nanowire configurations. Single nanowires and an array of three parallel nanowires separated by nanogaps have been investigated. Finite element method (FEM) simulations have been used to determine the plasmonic response of metallic nanostructures to incident electromagnetic waves. The FEM is a numerical technique used to solve partial differential equations with a given set of boundary conditions. The domain of the simulation is divided into many discrete pieces, known as finite elements. To approximate the total solution, the partial differential equations are solved in each finite element and the solutions are combined.²² The simulations are performed in a two-dimensional simulation space, which approximates the nanowires as infinitely long with a rectangular cross-section (shown meshed in Fig. 2 and post-simulation in Fig. 3(b)). The top edges of the cross-section are beveled to provide a closer approximation to an actual nanowire. To separate the domain of the simulation into finite elements, the nanowire geometry and surrounding medium are meshed using a free triangular mesh, which is shown in Fig. 2.

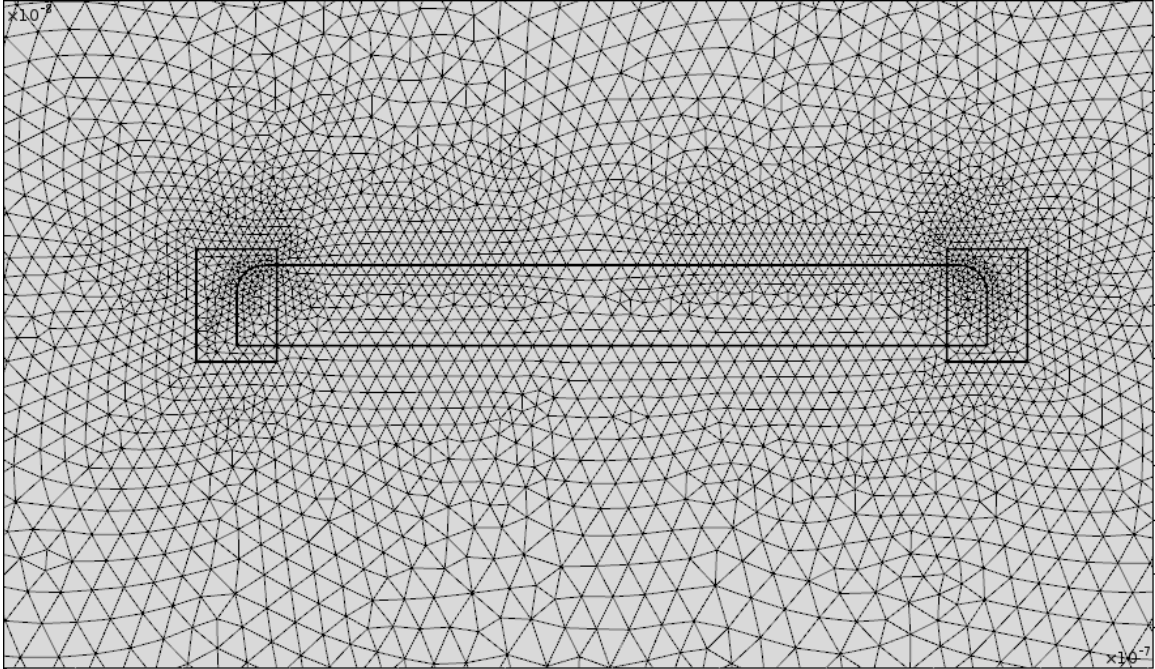


Fig. 2 A screenshot displaying the mesh used to perform FEM simulations of a single 2D gold nanowire. The area surrounding the nanowire geometry is the far field domain. The darker rectangles surrounding the edges of the nanowire are included to allow the calculation of average enhancement inside, but are not used in this paper.

Substrate effects have been approximated by using an effective medium of $n_{eff} = 1.25$ in the space surrounding the nanowires^{9,15}. The material properties of gold are applied to the nanowires and are modeled using an experimentally derived dielectric function.²³ An electromagnetic wave is incident with the k -vector perpendicular to the top surface of the nanowire and is transversely polarized (the electric field is polarized across the width of the nanowire) for each simulation. Surrounding the nanowire geometries is a circle of radius 1100 nm, split into two distinct layers: the far field domain, an 800 nm radius inner layer, and a perfectly matched layer (PML), a 300 nm outer layer. The far field domain represents the air through which the electromagnetic wave propagates before it contacts the nanowires. The effective medium is applied to the far field domain to model the properties of air along with the substrate. The purpose of the PML is to absorb light that

has been scattered from the nanowire geometry and prevent it from scattering back into the simulation space to provide more accurate results by reducing noise.

2.2 Interpreting Results

Each simulation reports a plot of the electric field distribution (EFD), defined as E/E_0 , where E is the local electric field at a given point near the plasmonic nanostructure and E_0 is the incident electric field. Therefore, the EFD is the ratio of the local electric field to the incident electric field. A number also of interest is the optical enhancement, defined as E^2/E_0^2 (or the EFD squared), which is a measure of the increase in local intensity, as intensity I is proportional to the electric field squared: $I \propto E^2$.

When enhancement values are reported in this work, they represent the maximum enhancement value for a particular simulation. The maximum enhancement value is found using an integration function within the simulation. The integration is performed over the entire simulation space, and reports the enhancement maxima for each unique simulation. The maximum enhancement is located in the region close to the nanowire sidewalls, as seen in Fig. 3(b).

CHAPTER 3:

RESULTS

3.1 Single Nanowire Width Dependence

First the dependence of enhancement on the width of the nanowire was determined. Enhancement spectra for various widths are plotted in Figure 3(a). These are the maximum optical enhancement of a single gold nanowire as a function of the wavelength of the light incident on the structure. Each line on the plot represents a different simulation for a particular width. The lines are separated by the step size indicated on the plot for clarity. The width ranges from 40 nm to 140 nm, with a step size of 5 nm between each line. It can be clearly seen that the enhancement peak shifts toward the red as nanowire width increases. Figure 3(b) is an accompanying set of electric field distributions to demonstrate the enhancement patterns that arise for single nanowires. The plots in Fig. 3(b) are from simulations of varying widths for an incident wavelength of 700 nm. The lines corresponding to each electric field distribution are linked with blue lines.

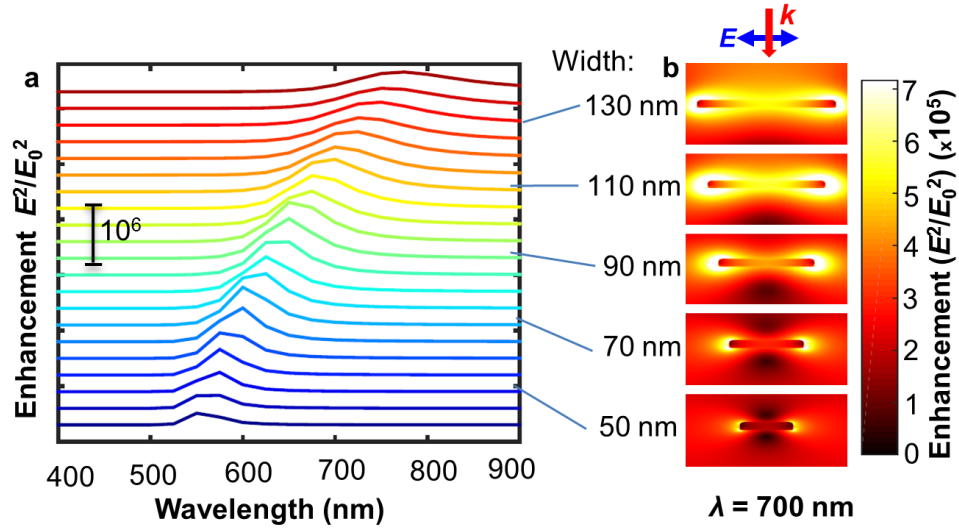


Fig. 3 (a) Enhancement spectrum and (b) electric field distributions for single gold nanowires of varying widths.

Figure 4(a) plots the incident wavelength that provides the maximum optical enhancement for a particular nanowire width. The graph shows a linearly increasing relationship between the wavelength providing maximum enhancement and nanowire width. The errors bars display an error of 25 nm above and below each point due to the 25 nm step size of wavelength between simulations. Figure 4(b) plots the full width at half maximum (FWHM) of the broadening in the enhancement spectrum as nanowire width increases. As can be seen from the plot, the broadening exhibits a quadratic proportionality to the width of the nanowire.

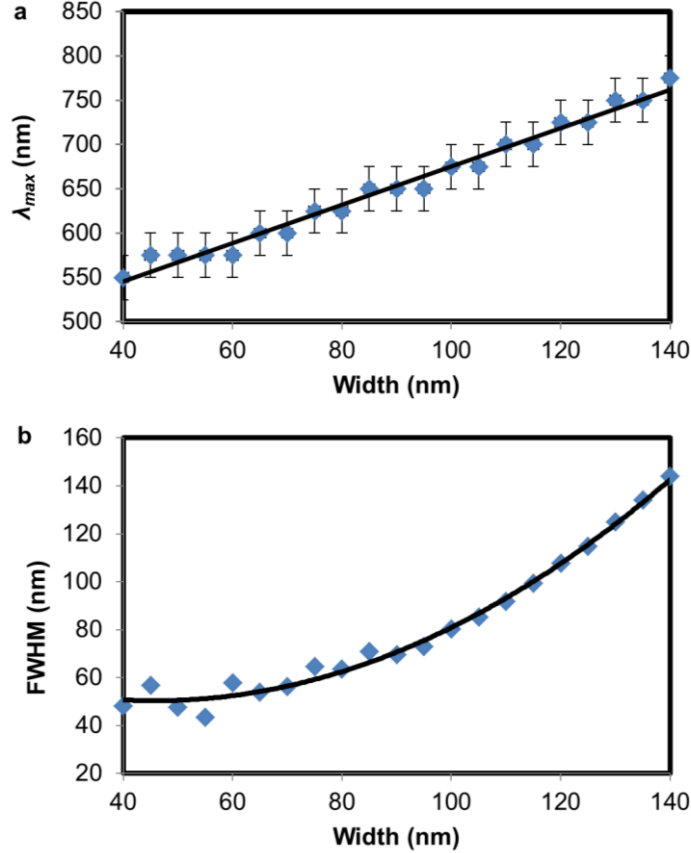


Fig. 4 (a) Wavelength of maximum enhancement and (b) FWHM of enhancement spectrum as functions of width for a single nanowire.

3.2 Triple Nanowire Array

The next simulations model three nanowires in parallel separated by nanogaps. The motivation for this structure is due to a unique geometry that can be fabricated by the nanomasking technique.²⁴ Figure 5(a) demonstrates the naming convention used in this paper when varying the geometry of a triple nanowire array. The outer nanowires have the same width, denoted w_s , while the width of the center nanowire is denoted w_L . Figures 5(b-d) are electric field distributions for several unique simulations. For the three simulations shown, the incident wavelength, gap width and nanowire thickness remain constant at values of 700 nm, 5 nm and 15 nm, respectively. The difference between each simulation is the widths of the nanowires, indicated at the top of each electric field

distribution. From the figure, one can see that the optical enhancement is concentrated in the gaps between the nanowires, and also at the corners of each nanowire. Another observation of significance is the substantial difference in gap enhancement for varying nanowire widths, such as seen between Fig. 5(b) and Fig. 5(d). In this case, a substantial increase (from 5(d) to 5(b)) in optical enhancement is seen for a difference in w_s of only 20 nm.

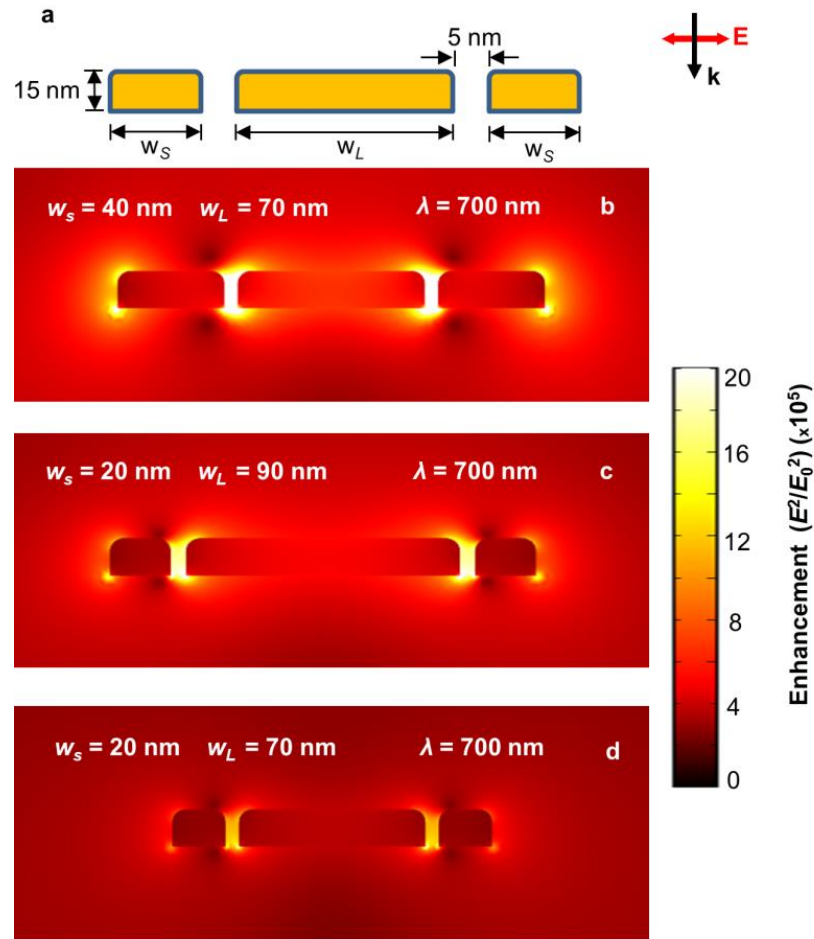


Fig. 5 (a) Triple nanowire array geometry, (b-d) enhancement distributions of triple nanowire arrays with various geometries.

Figures 6(a-d) plot the maximum optical enhancement for each unique w_s and w_L combination for incident wavelengths of 600 nm, 700 nm, 800 nm and 900 nm. The

width w_s ranges from 10 nm to 90 nm while w_L ranges from 40 nm to 140 nm, both with a step size of 10 nm. The intensity profile follows a roughly negative linear pattern for all wavelengths.

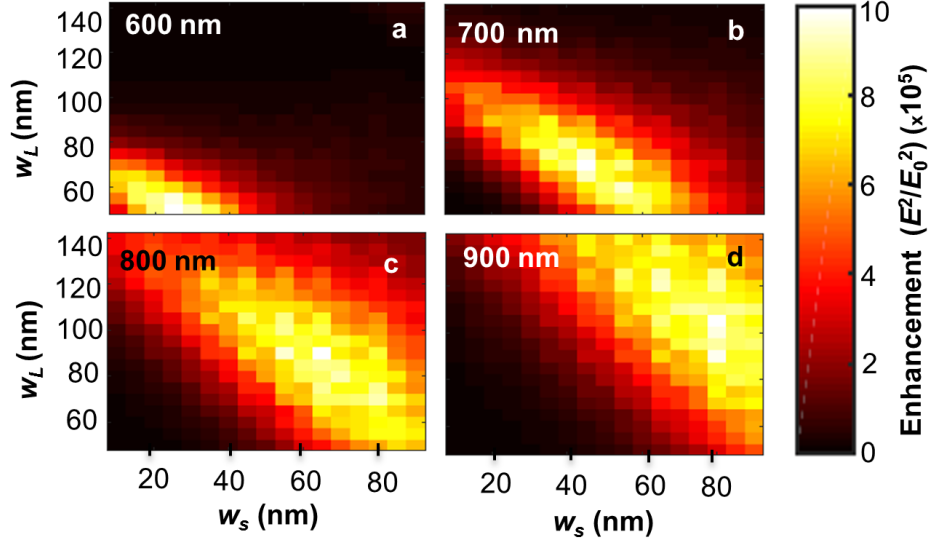


Fig. 6 Maximum enhancement of triple nanowire array as a function of w_s and w_L for triple nanowire array.

Figure 7(a) plots the maximum optical enhancement that was obtained as w_L was varied as a function of w_s . It can be seen from the plot that the peak of the optical enhancement curves strongly shifts to higher w_s for increasing wavelength. Figure 7(b) plots the w_L that provides the maximum optical enhancement as a function of w_s . The ranges of points plotted differ for each wavelength due to shifts in the enhancement patterns that can be seen in Fig. 6(a-d). The slope values obtained for 600 nm, 700 nm, 800 nm and 900 nm wavelengths are -0.9, -0.9818, -0.9755 and -0.8667 with vertical intercept (b_i) 72 nm, 113 nm, 147 nm, and 173 nm, respectively. In order to develop a general equation to determine the optimal w_L for maximum enhancement based on wavelength and w_s , a general function

$$w_L = f(w_s, \lambda) \quad (1)$$

was considered. Based on the similarity in slope between each line, and the roughly linear relationship between their vertical intercepts, the general function can be rewritten as

$$w_L = \langle m \rangle w_s + b_L(\lambda) \quad (2)$$

where $\langle m \rangle$ is the average slope of the enhancement for each spectra and $b_L(\lambda)$ is calculated from the vertical intercept values b_i . The vertical intercept as a function of wavelength is given by: $b_L(\lambda) = \frac{\Delta b}{\Delta \lambda} \lambda + C$, where $\frac{\Delta b}{\Delta \lambda} = 0.0337$ and the constant $C = -126.5$ nm is extrapolated from observed values. Plugging the calculated values into Eq. 1, one obtains:

$$w_L = -0.931w_s + 0.337\lambda - 126.5 \text{ nm}. \quad (3)$$

The solid lines in Fig. 6(b) are plots of Equation 3 for each wavelength. Equation 3 is a useful result that can be used to design a structure with appropriate parameters (w_L , w_s or λ) to the optimum value to maximize the optical enhancement of a gold nanowire array if the other two variables are defined. As can be seen in Fig. 7(b), Eq. 3 is a good estimation of the optimum value of w_L for the plotted data.

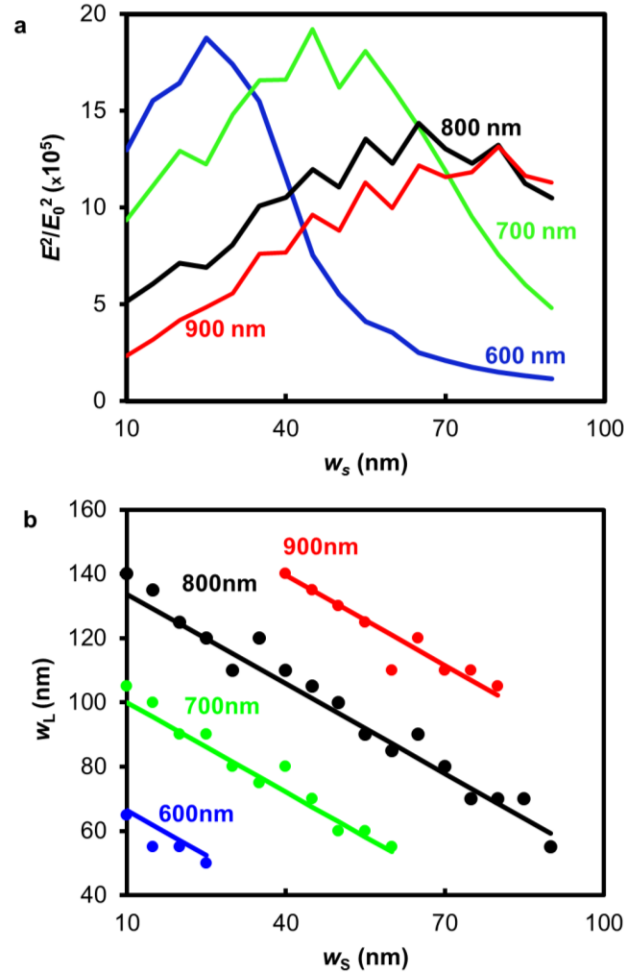


Fig. 7 (a) Maximum optical enhancement as a function of w_s and (b) w_L as a function of w_s for triple nanowire array.

3.3 Thickness Dependence

Figures 8(a-d) correspond to simulations of a single nanowire, and plot the maximum optical enhancement as a function of nanowire thickness and width for incident wavelengths of 600 nm, 700 nm, 800 nm and 900 nm. It can be clearly seen that these color plots exhibit a significantly different enhancement pattern shift than those shown for the triple nanowire array in Fig. 6(a-d). The slope of the maximum enhancement line changes significantly between each wavelength, and is positive rather than negative.

Additionally, as wavelength increases, the maximum enhancement at lower nanowire thickness shifts to the right toward higher widths.

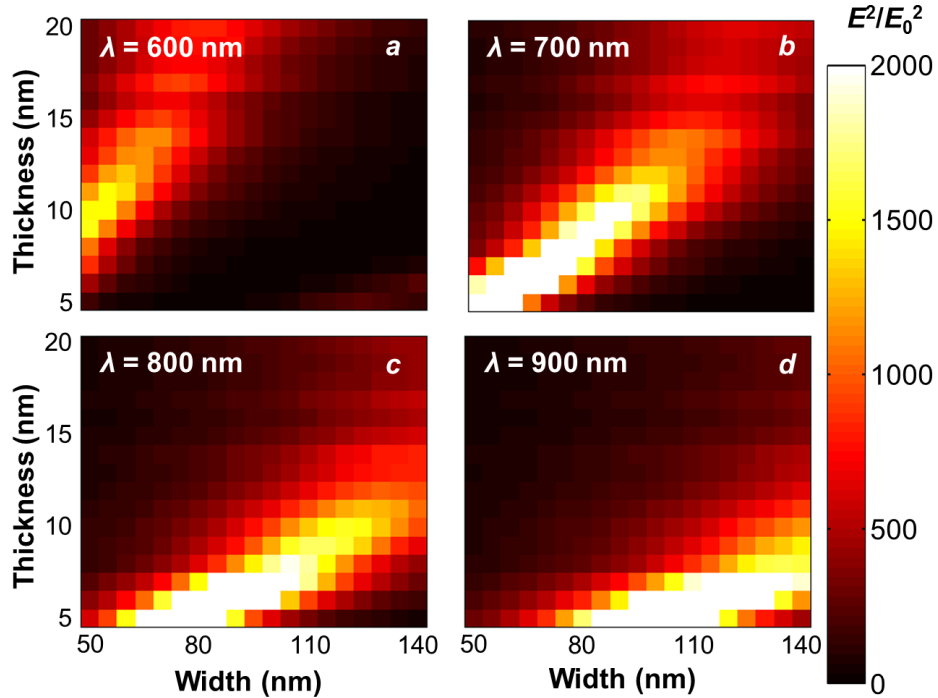


Fig. 8 Maximum optical enhancement as a function of width and thickness for a single nanowire.

Figure 9(a) plots information similar to Fig. 7(b), but instead plots the thickness that provides the maximum enhancement as a function of width. Again, the range of points on each line is different due to shifts in the enhancement pattern that can be seen in Fig. 8(a-d). Figure 9(a) more clearly demonstrates the shift in the slope of the enhancement pattern between each wavelength. The slope values obtained for 600 nm, 700 nm, 800 nm and 900 nm wavelengths are 0.2854, 0.1674, 0.0992, and 0.0789, respectively. Using the same method as for the first equation, the first step in developing a general equation is

$$t = f(w, \lambda) \quad (4)$$

where t is the nanowire thickness, w is the nanowire width and λ is the incident wavelength. Since the slope is different for each wavelength, it must be represented as a function of wavelength rather than an average:

$$t = m(\lambda) \cdot w + b \quad (5)$$

where b is an intercept interpolated from the data. The slope as a function of wavelength is given by: $m(\lambda) = \frac{\Delta m}{\Delta \lambda} \lambda + C$, where $\frac{\Delta m}{\Delta \lambda} = -0.0007$ and the constant $C = 0.6735$ is extrapolated from observed values. Combining the above values with Eq. 5 yields:

$$t = \left(-0.0007 \frac{1}{\text{nm}} \cdot \lambda + 0.6735 \right) \cdot w + b_i \text{ nm.} \quad (6)$$

In Eq. (6), b_i is a constant that differs between wavelengths, and is adjusted between -1 and 5 nm to fit Eq. (6) to the data. The solid lines in Fig. 9(a) are plotted using Eq. 6. Again, another useful relationship between t , w , and λ has been determined. This result can be used to optimize the design parameters to maximize the optical enhancement of a single gold nanowire. Figure 9(b) plots the maximum enhancement for each width, where the thickness is the one that provides the highest enhancement for the given width. The plot shows that the maximum optical enhancement peak shifts to the right for increasing wavelength, in a fairly consistent step size of ~25 nm.

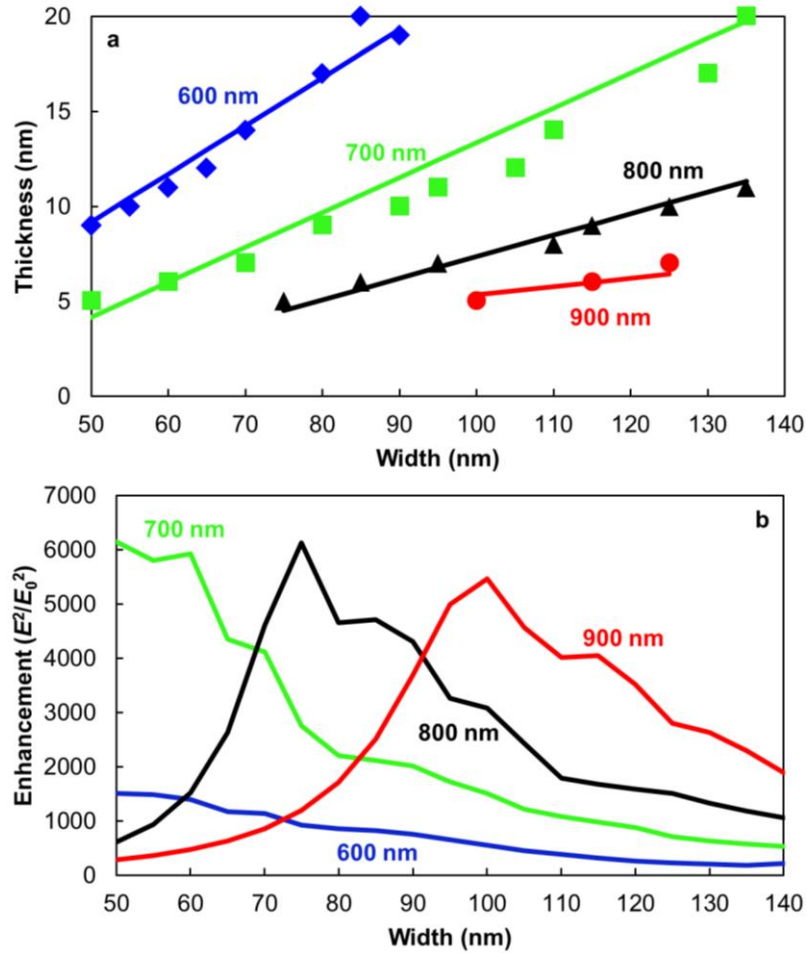


Fig. 9 (a) Thickness showing maximum enhancement as a function of width and (b) maximum enhancement as a function of width.

Figure 10 displays simulation results in the form of electric field distributions, each corresponding to a different nanowire thickness. For each simulation, the wavelength and nanowire width remain constant at 700 nm and 100 nm, respectively. These plots show that there is a significant difference in optical enhancement between simulations, as can most clearly be seen between the electric field distributions for nanowire thicknesses of 5 nm and 11 nm.

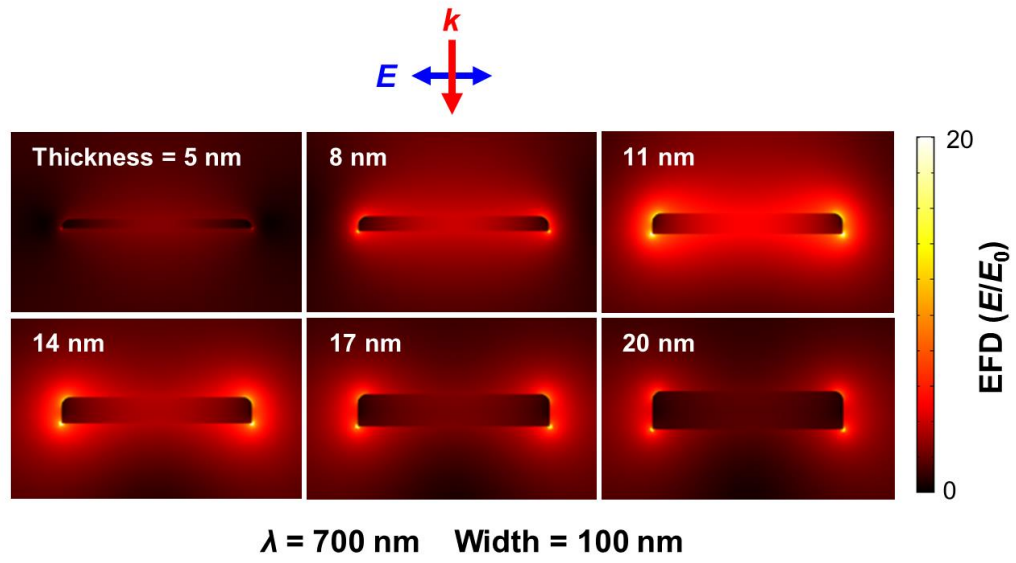


Fig. 10 Electric field distributions of single nanowires of varying thickness.

CHAPTER 4: CONCLUSION

This work investigated the optical enhancement properties of gold nanowires in two dimensions using finite element method analysis. By varying the geometry of the wires, for a single-direction transversely polarized electromagnetic wave, the plasmonic coupling was tuned in the visible spectrum for a single gold nanowire and triple gold nanowire arrays. From the simulation results, it can be seen that single nanowires and triple nanowire arrays exhibit a significant effect of incident wavelength and nanowire geometry on their maximum possible optical enhancement. This serves as a preliminary investigation of the effect of nanowire thickness on optical enhancement and the ideal dimensions for triple nanowire arrays that are currently being manufactured in our lab for optical characterization. The relationship between these parameters has been found for the tested geometries (Eqs. (3) and (6)) and can serve as a useful tool to researchers as they design and fabricate plasmonic nanostructures.

As the control provided by various nanostructure fabrication methods advances, it will become necessary to appropriately tune the geometry of plasmonic nanostructures in order to maximize their effectiveness in any given application, as has been demonstrated in previous work^{18,20}. Therefore, future work will be focused on fabrication of the structures detailed in this paper to verify the results of the simulations. Also necessary is a continuation of the simulation models, to provide a higher number of data points for a wider variety of plasmonic structures. A higher number of data points will both verify the existing data and allow for more accurate equations to be formulated.

APPENDIX A:

PERFORMING A NANOWIRE SIMULATION IN COMSOL

Beginning a Model

1. From the Model Wizard, select 2D.
2. In the select physics tree, selects Optics – Wave Optics – Electromagnetic Waves, Frequency Domain, click add.
3. Click on Study, select Preset Studies – Frequency Domain, click done.

Parameters

1. Click on Parameters, locate the Parameters section.
2. Enter the following parameters:

Name	Expression	Description
lda	600[nm]	Wavelength
f0	c_const/lda	Frequency
t_air	800[nm]	Thickness of air layer
t_pml	300[nm]	Thickness of PML
h_max	25[nm]	Maximum element size
neff	1.25	Effective medium refractive index
k0	$2*\pi/lda$	
width	140[nm]	Width of rectangle
height	15[nm]	Height of rectangle

3. Right click Definitions and choose Functions – Interpolation.
4. Choose file from the data source list, locate the eps real gold data list, click Import.
5. Name the function eps_real; in the Units section, Arguments field, type Hz.
6. In the function field, type 1.
7. Repeat steps 6-9 for the eps imaginary data list, and name it eps_imag instead.

Geometry

1. Under Component 1, right click Geometry and choose Circle.
2. In the Circle settings window, set the radius to $t_{\text{air}}+t_{\text{pml}}$ and the sector angle to 360.
3. In the Layers section, add a layer with the name Layer 1 and a thickness of t_{pml} .
4. Press the Build Selected button.
5. Right click Geometry and choose Rectangle.
6. In the Rectangle settings window, in the Width box type width and in the Height box type height.
7. Press the Build Selected button.
8. Right click Geometry and click Fillet.
9. Select the top two corners of the rectangle in the vertices to fillet box, and in the Radius box type $5[\text{nm}]$.
10. Press the Build Selected button.

Definitions

1. Right click Definitions and select Perfectly Matched Layer.
2. Use the Domain Selection box to select the outermost Layer of the sphere surrounding the nanowire.
3. Under Scaling set the Typical wavelength from box to user defined.
4. Under Typical wavelength, type $l_{\text{da}}/n_{\text{eff}}$.
5. Right click Definitions and select Component Couplings – Maximum
6. In the Operator name box type max_Enorm .
7. In the Source Selection box, select the domain surrounding the nanowire.
8. Right click Definitions and select Variables.

9. Add a variable named max with an expression of $(\max_E_{\text{norm}}(\text{emw.NormE}))^2$.

Materials

1. Right click Materials, and select Add Material.
2. Label the material Air, select all domains in the Geometric Entity Selection box.
3. In the Material Contents Box, add Relative permeability, Relative permittivity and Electrical conductivity if they are not present using the material properties lists.
4. Set Relative permeability to 1, Relative permittivity to n_{eff}^2 and Electrical conductivity to 0.
5. Right click Materials, and select Add Material.
6. Label the material Gold, select the domains representing the nanowire only.
7. Add the same Material Properties as for Air.
8. Set Relative permeability to 1, Relative permittivity to $\text{AuReal}(l_{\text{da}}) - i * \text{AuImag}(l_{\text{da}})$ and Electrical conductivity to 0.

Electromagnetic Waves, Frequency Domain

1. Click Electromagnetic Waves, Frequency Domain
2. In the Solve for list, choose Scattered field.
3. In the E_b field, type:

$\text{Exp}(-i * n_{\text{eff}} * k_0 * -y)$	x
0	y
0	z

4. Right click Electromagnetic Waves, Frequency Domain, select Wave Equation, Electric.
5. Under Wave Equation, Electric 1, set each component to be From material.

Meshes

1. Right click Mesh and select Size.
2. Input the following parameters:

Maximum element size	h_max
Minimum element size	3.9E-10
Maximum element growth rate	1.1
Curvature factor	0.3
Resolution of narrow regions	1

3. Right click Mesh and select Free Triangular.
4. In the Domain Selection box, select everything but the PML.
5. Right click Mesh and select Mapped.
6. In the Domain Selection box, select the PML.
7. Click Mesh and select Build All.

Study I

1. Right click Study 1 and choose Parametric Sweep.
2. Click the Add button twice.
3. Input the following settings:

height	range(5[nm],1[nm],20[nm])
width	range(50[nm],5[nm],140[nm])

4. Click Step I: Frequency Domain.
5. In the Frequencies field, type f0.
6. Click Study I.
7. In the Study Settings section, clear the Generate default plots check box.

Results

1. Right click Derived Values and select Surface Maximum.
2. In the Selection box, select all domains.

3. In the Expression field, type max.

To perform a study, right click on Study 1 and click Compute.

APPENDIX B:

MATLAB CODE USED TO GENERATE COLOR PLOTS

```
A = [  
]; %creates a matrix of data, separate rows with a semicolon  
  
imagesc(A) %creates an image plot of the matrix A  
colormap(hot) %changes the color range used by the color plot  
caxis([0 2000]) %sets the range of the color bar  
colorbar %displays the color bar  
axis equal tight %gives the final image plot a square shape  
xlabel('Width (nm)') %labels the x-axis  
ylabel('Thickness (nm)') %labels the y-axis  
title('\lambda = 600nm') %titles the image plot  
set(gca, 'XTick', 1:19, ... %sets number of ticks on x-axis  
  
'XTickLabel', {'50', '', '', '', '', '', '80', '', '', '', '', '', '110', '', '', '', ''  
, '', '140'}, ... %sets labels for each tick on x-axis, '' signifies a  
blank space  
'YTick', 1:16, ... %sets number of ticks on y-axis  
  
'YTickLabel', {'20', '', '', '', '', '', '15', '', '', '', '', '10', '', '', '', '', '5'}, ..  
.. %sets labels for each tick on y-axis, '' signifies a blank space  
    'TickLength', [0 0]); %leave as is
```


BIBLIOGRAPHY

1. J. B. Pendry, et al., “Extremely Low Frequency Plasmons in Metallic Mesostructures,” *Phys. Rev. Lett.* **76** (25), pp 4773–4776 (1996).
2. S. A. Maier, *Plasmonics: Fundamentals and Applications*. Springer Science+Business Media LLC (2007).
3. C. M. Cobley, et al., “Gold nanostructures: a class of multifunctional materials for biomedical applications,” *Chem. Soc. Rev.* **40**, pp 44-56 (2011).
4. D. K. Gramotnev and S. I. Bozhevolnyi, “Plasmonics beyond the diffraction limit,” *Nature Photon.* **4**, pp 83-91 (2010).
5. H. Wei, et al., “Polarization dependence of surface-enhanced raman scattering in gold nanoparticle-nanowire systems,” *Nano Lett.* **8** (8), pp 2497–2502 (2008).
6. H. A. Atwater and A. Polman, “Plasmonics for improved photovoltaic devices,” *Nature Mater.* **9**, pp 205-213 (2010).
7. E. T. Yu, et al., “Plasmonic nanoparticle scattering for enhanced performance of photovoltaic and photodetector devices,” *Proc. SPIE* **7033** (2008).
8. J. N. Anker, et al., “Biosensing with plasmonic nanosensors,” *Nature Mater.* **7**, pp 442-453 (2008).
9. J. B. Herzog, et al., “Dark Plasmons in Hot Spot Generation and Polarization in Interelectrode Nanoscale Junctions,” *Nano Lett.* **13**(3), 1359-1364 (2013).
10. W. Wu, A. Bonakdar and H. Mohseni, “Plasmonic enhanced quantum well infrared photodetector with high detectivity,” *App. Phys. Lett.* **96**, 161107 (2010).
11. A. M. Hill, et al., “Computational electromagnetic analysis of plasmonic effects in interdigital photodetectors,” *Proc. SPIE* **9163** (2014).
12. A. I. Nusir, et al., “Near-infrared metal-semiconductor-metal photodetector based on semi-insulating GaAs and interdigital electrodes,” *Photon. Res.* **3**, pp 1-4 (2015).
13. M. Zhu, et al., “Micropatterning Thermoplasmonic Gold Nanoarrays To Manipulate Cell Adhesion,” *ACS Nano* **6**(8), pp 7227-7233 (2012).
14. R. Rodríguez-Oliveros and J. A. Sánchez-Gil, “Gold nanostars as thermoplasmonic nanoparticles for optical heating,” *Opt. Express* **20**, pp 621-626 (2012).
15. J. B. Herzog, et al., “Thermoplasmonics: Quantifying Plasmonic Heating in Single Nanowires,” *Nano Lett.* **14**(2), 499-503 (2014).

16. X. Huang, et al., "Plasmonic photothermal therapy (PPTT) using gold nanoparticles," *Lasers Med. Sci.* **23**, pp 217-228 (2008).
17. X. Huang and M. A. El-Sayed, "Plasmonic photo-thermal therapy (PPTT)," *Alex. J. of Med.* **47**, pp 1-9 (2011).
18. M. A. Mackey, et al., "The Most Effective Gold Nanorod Size for Plasmonic Photothermal Therapy: Theory and *In Vitro* Experiments," *J. Phys. Chem. B* **118**, pp 1319-1326 (2014).
19. Y. H. Wang, et al., "Synergistic delivery of gold nanorods using multifunctional microbubbles for enhanced plasmonic photothermal therapy," *Sci. Rep.* **4**, pp 1-8 (2014).
20. S. Yun, et al., "Linker-Molecule-Free Gold Nanorod Films: Effect of Nanorod Size on Surface Enhanced Raman Scattering," *J. Phys. Chem. C* **2009**, pp 13551-13557 (2009).
21. D. Natelson, Y. Li, and J. B. Herzog, "Nanogap structures: combining enhanced Raman spectroscopy and electronic transport," *Phys. Chem. Chem. Phys.* **15**, pp 5262-5275 (2013).
22. A. C. Polycarpou, *Introduction to the Finite Element Method in Electromagnetics*. Morgan & Claypool Publishers (2006).
23. P. B. Johnson and R. W. Christy, "Optical Constants of the Noble Metals," *Phys. Rev. B* **6**, pp 4370-4379 (1972).
24. J.B. Herzog and D. Natelson, U.S. Patent Application No. 62,039,337 (2014).